Građevinski materijali i konstrukcije
Building Materials and Structures

journal homepage: www.buildingmaterialsstructures.com

https://doi.org/10.5937/GRMK2600001O UDK: 624.151.5:624.046.2
624.131.526:552.52

Original scientific paper

Numerical prediction of bearing capacity and settlement of shallow foundation on overconsolidated clays using the Hardening State Parameter model

Nikola Obradović[1)], Sanja Jocković[*1)]

[1)] *University of Belgrade, Faculty of Civil Engineering, Belgrade, Serbia*

Article history

Received: 03 November 2025
Received in revised form:
17 December 2025
Accepted: 24 December 2025
Available online: 30 January 2026

Keywords

bearing capacity,
settlement,
shallow foundations,
PLAXIS 2D,
HASP,
overconsolidated clay

ABSTRACT

A numerical analysis was performed to investigate the bearing capacity and settlement behaviour of shallow foundations on overconsolidated clays. Finite element analyses were conducted in PLAXIS 2D using two constitutive soil models: the Modified Cam Clay and the Hardening State Parameter (HASP) model. The HASP model, implemented as a user-defined constitutive formulation, introduces state-dependent hardening within the critical state framework to represent the stress-strain behaviour of overconsolidated clays. The study reproduced field load tests on two shallow footings (A and B) at the Bothkennar research site, supported by comprehensive measurements of settlements and pore-water pressures. All soil parameters were adopted directly from published laboratory data, without further calibration. The analyses focused on the load-displacement response, time-dependent settlements under sustained loading, and the development and dissipation of excess pore-water pressures. The HASP model provided a realistic prediction of the measured field behaviour, showing good agreement with observations and demonstrating its capability to capture the coupled hydro-mechanical response of overconsolidated clays.

1 Introduction

In many natural deposits, the upper clay layers have undergone significant preloading and subsequent unloading, producing overconsolidated materials whose stiffness, strength, and volumetric response differ significantly from those of normally consolidated clays. Upon reloading, overconsolidated clays respond with a stiffness nonlinearity and early plastic deformation, while the volumetric tendency often evolves from compression to dilation as shearing develops. The observed behaviour has been widely documented through laboratory studies and in-situ tests, demonstrating dependencies on the overconsolidation ratio, structure, and stress path [1-5]. The interplay between structure degradation, pore pressure response, and dilatancy governs the load-displacement behaviour of shallow foundations, controlling both the mobilization of bearing resistance and post-peak softening. Consequently, reliable prediction of foundation performance demands constitutive models capable of reproducing these path-dependent mechanisms and the associated evolution of stress-strain behaviour [6-10].

Traditional analytical formulations for evaluating the bearing capacity and settlement of shallow foundations provide useful design frameworks, but rely on idealized representations of soil behaviour and failure mechanisms that rarely reflect field conditions. These methods typically idealize the soil as a homogeneous and isotropic material that behaves elastically up to failure, adopting rigid-plastic or elastic-perfectly plastic assumptions and simplified failure mechanisms. The conventional analysis of shallow foundations further separates the problem into two distinct calculations: one for bearing capacity, in which the soil is treated as a rigid-perfectly plastic material, and another for settlement, in which the soil is assumed to behave as a linear or slightly non-linear elastic continuum. Such formulations neglect the gradual onset of plastic strains, stiffness degradation, and pore-pressure evolution that arise from coupled hydro-mechanical processes in overconsolidated clays, and they often lead to either overestimation or underestimation of the actual soil behaviour [6, 9, 11].

In contrast, numerical methods based on the finite element or meshfree frameworks, when coupled with advanced constitutive models enable a more realistic representation of soil behaviour under loading. They can simulate the progressive yielding, dilation, and pore-pressure dissipation that control both bearing resistance and long-term settlement. Hence, contemporary research supports the transition from purely analytical solutions toward fully coupled numerical analyses for the design of shallow foundations on overconsolidated clays [5, 7, 8, 11, 12, 13]. The accuracy of numerical predictions in geotechnical analysis strongly depends on the choice of the constitutive model, as it defines how soil stiffness, strength,

[*] Corresponding author:
E-mail address: borovina@grf.bg.ac.rs

and volumetric behaviour evolve under loading. Early models such as the Mohr-Coulomb (linear elastic-perfectly plastic) provide only a crude approximation of real soil response, as they cannot reproduce strain-dependent stiffness, dilatancy, or stress-path effects that are characteristic of overconsolidated clays [4]. The adoption of critical state-based models, particularly the Modified Cam Clay (MCC) framework [14, 15], represented a significant advancement by introducing a yield surface that evolves with plastic volumetric strain and stress history. However, since the MCC model was developed to represent normally consolidated clays, it cannot adequately capture the complex behaviour of overconsolidated soils. To overcome numerous shortcomings, several enhanced models have been developed. These models are generally based on the MCC concept and can be grouped according to two main theoretical approaches: the *Multi-Surface Plasticity* (MSP) and the *Bounding Surface Plasticity* (BSP) frameworks. Representative MSP-type models include the Bubble model proposed by Al-Tabbaa and Wood [16], the MIT-E3 model by Whittle and Kavvadas [17], and the 3-SKH model by Stallebrass and Taylor [18], later refined by Gajo and Wood [19]. Within the BSP family, well-known formulations are the CASM model [20], the Modified 3-SKH model [21], the SANICLAY model [22], and the UH model [23]. Each of these models represents a step forward in capturing the effects of the overconsolidation ratio, stress and strain history, and anisotropy that govern the stress-strain behaviour of natural clays.

In this paper, the Hardening State Parameter (HASP) model [24, 25] was adopted to simulate the behaviour of overconsolidated clays beneath shallow foundations. The model was implemented as a User-Defined Soil Model (UDSM) in PLAXIS 2D [26]. The numerical analyses were performed on the well-documented case study of two shallow footings (Footings A and B) investigated by Freitas et al. [8], where extensive laboratory and field measurements are available. The results obtained with the HASP model were compared with those predicted by the MCC model, from which HASP was originally derived, in order to assess the improvements achieved by incorporating state-dependent hardening.

2 HASP constitutive model

The HASP model is a critical-state bounding surface constitutive model developed to describe the behaviour of overconsolidated clays over a wide range of overconsolidation ratios. It retains the simplicity and parameter set of the MCC model while offering a more realistic representation of clay behaviour. Within the bounding surface plasticity framework, the HASP model defines the yield surface through the current stress point, enabling elasto-plastic behaviour from the onset of loading. The HASP model is formulated in triaxial $q - p'$ plane, where p' is the mean effective stress and q is the deviatoric stress. Its main innovation lies in a hardening rule expressed through a state parameter that links the current and conjugate stress points on the yield (A) and bounding surfaces $(\overline{A})$ (Figure 1) allowing the simultaneous reproduction of strain hardening, peak strength, and subsequent softening.

The yield and bounding surfaces (Figure 1) are defined by:

$$F(p', q) = \left(\frac{q}{M}\right)^2 + p'(p' - p'_0) \tag{1}$$

$$\bar{F}(\bar{p}', \bar{q}) = \left(\frac{\bar{q}}{M}\right)^2 + \bar{p}'(\bar{p}' - \bar{p}'_0) \tag{2}$$

where M is the gradient of the critical state line in the $q - p'$ plane and p'_0 is the maximum mean effective stress defining the size of the yield surface. The hardening rule is formulated as a function of plastic volumetric and plastic shear strain and can be expressed through the hardening coefficient ω, where the effect of dilatancy is implicitly included via the ratio

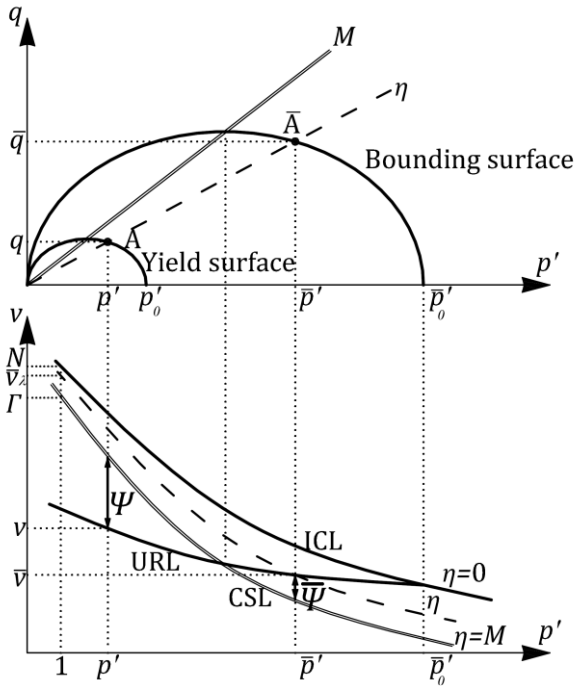

Figure 1. HASP model, stress plane and state parameters [25]

of plastic shear to plastic volumetric strain increments, $d\varepsilon_q^p/d\varepsilon_v^p$:

$$dp_0' = \frac{v}{\lambda-\kappa}p_0'\left(d\varepsilon_v^p + \xi d\varepsilon_q^p\right) = \frac{v}{\lambda-\kappa}p_0' d\varepsilon_v^p \omega \tag{3}$$

where v is specific volume, λ is the slope of the virgin compression line (VCL), κ is the slope of a swelling line (URL) in the $v - lnp'$ plane. The hardening coefficient ω is defined in terms of the state parameter at the current stress point Ψ, the state parameter at the conjugate point on the bounding surface $\bar{\Psi}$ (Figure 1), and the overconsolidation ratio R, as:

$$\omega = \left(1 + \frac{\bar{\Psi} - \Psi}{\bar{\Psi}}\right)R \tag{4}$$

The state parameters are given by:

$$\Psi = v + \lambda\, ln\, p' - \Gamma \tag{5}$$

$$\bar{\Psi} = (\lambda - \kappa)\, ln\left(\frac{2M^2}{M^2 + \eta^2}\right) \tag{6}$$

where Γ is specific volume at $p' = 1\ kPa$ on the critical state line. The overconsolidation ratio R, relating the current stress point to its conjugate point on the bounding surface, is defined as:

$$R = \frac{\bar{p}'}{p'} = \frac{\bar{q}}{q} = exp\left(\frac{\bar{\Psi} - \Psi}{\lambda - \kappa}\right) \tag{7}$$

Finally, complete constitutive relations of the HASP model are:

$$\begin{Bmatrix} d\varepsilon_v \\ d\varepsilon_q \end{Bmatrix} = \begin{bmatrix} \frac{1}{K} + \frac{\lambda-\kappa}{vp'\omega}\frac{M^2-\eta^2}{M^2+\eta^2} & \frac{\lambda-\kappa}{vp'\omega}\frac{2\eta}{M^2+\eta^2} \\ \frac{\lambda-\kappa}{vp'\omega}\frac{2\eta}{M^2+\eta^2} & \frac{1}{3G} + \frac{\lambda-\kappa}{vp'\omega}\frac{4\eta^2}{(M^2+\eta^2)(M^2-\eta^2)} \end{bmatrix} \begin{Bmatrix} dp' \\ dq \end{Bmatrix} \tag{8}$$

where $\eta = q/p'$ is the stress ratio. A constant value of Poisson's ratio μ is used. Bulk modulus K and shear modulus G are defined by:

$$K = \frac{vp'}{\kappa} \tag{9}$$

$$G = \frac{3(1-2\mu)}{2(1+\mu)}K \tag{10}$$

As can be seen, the hardening coefficient also acts as a reduction factor for the plastic strain increments. By combining volumetric and shear strain hardening, the model ensures a smooth transition from contractive to dilative response, while the hardening coefficient acts as a plastic strain reduction factor, maintaining numerical stability even under small stress increments. All details and expressions can be found in [13, 24-27].

The HASP model requires only a few basic material and state parameters: compression index λ and swelling index κ as consolidation parameters, drained strength parameter M, the Poisson's ratio μ as elastic parameter, and the void ratio e_0 as state parameter, all of which can be determined from standard laboratory tests. For normally consolidated clays, the HASP model reduces to the classical MCC model, while for overconsolidated states, it provides an improved representation of dilatancy and peak strength. The model is implemented in the finite element software PLAXIS 2D through the UDSM formulation using an explicit modified Euler scheme with automatic substepping and error control as the stress integration procedure [28]. Prior to the boundary-value analyses, the UDSM implementation was verified by single-element simulations reproducing triaxial loading paths in compression and extension under both drained and undrained conditions over a range of OCR. The HASP model has been validated against a broad set of published laboratory and field data, including triaxial tests for different OCR levels and well-documented embankment case histories with monitored settlements and pore pressures [13]. Validation results have demonstrated realistic predictions of stress-strain behaviour, pore pressures, and the transition from hardening to softening across different OCR levels. All details of the implementation procedure verification and constitutive model validation are provided in [24, 26].

3 Finite element modelling of the two shallow footings

The finite element analyses were performed to simulate the short-term and long-term load-settlement behaviour of the two shallow footings tested at the Bothkennar research site, marked as Footings A and B. The numerical analyses were conducted to reproduce the field response and to assess the ability of the user defined constitutive model to capture the time-dependent behaviour of slightly overconsolidated natural clay. The subsoil conditions at the Bothkennar research site were well established through extensive site investigations [29, 30]. The groundwater table lies at approximately 0.9 m below the ground surface. The soil profile consists, from top to bottom, of recent tidal flat deposits, followed by a thin shell layer marking the unconformity with the underlying clay sequence, then a weathered crust, and finally the main body of Bothkennar clay, extending to a depth of about 20 m. The clay is lightly to moderately overconsolidated due to postglacial erosion and ageing effects.

Footing A (2.2 m × 2.2 m) was founded at a depth of 0.8 m. It was loaded in stages to failure over four days, reaching a maximum pressure of about 138 kPa. Footing B, slightly larger (2.4 m × 2.4 m), founded at the same depth, was tested one month later to study the long-term response of the same clay layer. After a short loading-unloading cycle, it was brought to a constant pressure of approximately 89 kPa (about two-thirds of the ultimate load from Footing A) and maintained under this load for around eleven years to observe consolidation and creep effects. Loading rates for both footings were the same. Both footings were instrumented to monitor settlements and pore-pressure changes in the underlying soil.

3.1 Numerical model

All numerical analyses were performed in PLAXIS 2D using a fully coupled flow-deformation formulation. Fifteen-node triangular elements were employed, which are a standard higher-order option in PLAXIS, proven to be robust for a wide range of geotechnical problems and better suited to capturing failure conditions. Both footings were idealized as axisymmetric circular foundations representing the same loaded area as the square pads tested in the field. The equivalent diameter of Footing A is 2.48 m, while that for footing B is 2.71 m. This simplification allowed an efficient numerical representation while maintaining realistic stress distribution beneath the foundation.

The model domain (Figure 2a) was extended sufficiently in both depth and lateral extent to minimize boundary effects. The base of the model was fixed in both horizontal and vertical directions, while the lateral boundaries were restrained horizontally but free vertically. Because both footings are symmetrical, only one half is modelled. The pore-water pressure boundary conditions were defined to represent realistic drainage behaviour of the foundation system. No flow was allowed along the axis of symmetry, while the bottom, top and right boundaries were assigned as drainage boundaries. The footing was modelled as an impervious material. The adopted finite element mesh is shown in Figure 2b. The meshing options were identical for both footings, resulting in identical meshes in the numerical models. For that reason, only the mesh for Footing A is presented. The numerical model for Footing A consisted of 1436 triangular elements, whereas that for Footing B consisted of 1431 elements. The footing was modelled with soil elements having the properties of concrete. The first stage of the numerical analysis simulated the excavation to the foundation level and concreting of the footing (i.e. the properties of elements representing the footing were changed from soil to concrete), followed by the application of the footing load, which was increased up to the specified magnitude. For Footing B, computation is then continued up to 11 years under constant load. The footings were loaded with a line load. The line load in the axisymmetric model has dimensions of surface load (kN/m/m). The soil above water table is allowed to sustain tensile pore water pressures to include suction in the calculation. Considering suction allows non-zero effective vertical stresses and a finite value of undrained strength at the ground surface.

3.2 Model parameters

In the numerical analyses, all soil layers were modelled using either the HASP model or the MCC model. No additional parameter calibration was performed for the constitutive models, and all input parameters were adopted directly from previously published laboratory data for Bothkennar clay [8]. The model parameters used in the analyses are summarized in Table 1. The model parameters for the MCC and HASP models are the same. Footings were modelled using a linear elastic constitutive model.

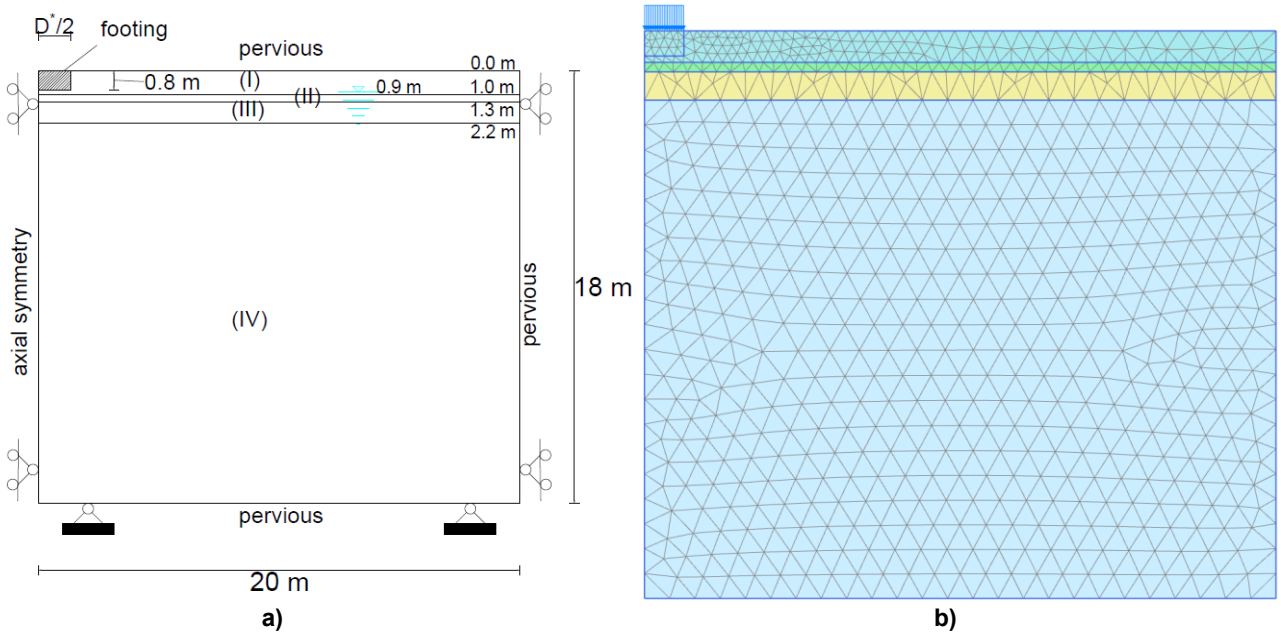

Figure 2. Computational domain (a) and finite element mesh (b)

Table 1. Numerical model and soil and footings parameters

Depth $[m]$	Soil strata	γ $[kN/m^3]$	μ $[-]$	e_0 $[-]$	POP $[kPa]$	OCR $[-]$	K_0^{NC} $[-]$	K_0^{OC} $[-]$	k $[m/s]$	MCC and HASP parameters κ $[-]$	λ $[-]$	M $[-]$
0.0-1.0	I	18.0	0.26	1.850	40	/	0.50	2.25	4.63×10^{-9}	0.03	0.24	1.462
1.0-1.3	II	17.0	0.26	1.850	40	/	0.50	1.620	1.00×10^{-8}			
1.3-2.2	III	17.0	0.26	1.85	35	/	0.50	1.0	4.63×10^{-9}			
2.2-18.0	IV	16.0	0.26	1.850	/	1.55	0.510	0.65	2.00×10^{-9}			
Footings		$\gamma = 25\ kN/m^3, E = 30\ GPa, \mu = 0.2$										

Variation of OCR and K_0^{OC} with depth is given in Figure 3. OCR values for layers (I), (II) and (III) are calculated using the equation:

$$OCR = \frac{\sigma_v' + POP}{\sigma_v'} \tag{11}$$

where σ_v' is vertical effective stress and POP is pre-overburden pressure. The preconsolidation of the upper three layers is set in the numerical model using the POP values given in Table 1. For the bottom layer (IV) a constant value of OCR by depth given in Table 1 is used. The coefficient of earth pressure at-rest for normally consolidated soil K_0^{NC} and overconsolidated soil K_0^{OC} for all soil layers has the same value as given in [8]. The hydraulic permeabilities in the horizontal and vertical directions are assumed to be equal, implying isotropic permeability. The permeability values remain constant throughout the calculation and are defined separately for each soil layer, as summarized in Table 1.

4 Results and discussion

The following sections present the results of the numerical analyses and their comparison with the field measurements. The results are shown for both the HASP and MCC models.

4.1 Load-displacement behaviour

The load-displacement curves obtained from the numerical analyses using the HASP and MCC models are compared with the measured field data for both Footings A and B, shown in Figures 4 and 5, respectively.

Both models reproduced the general trend of the load-settlement relationship observed in the field. The MCC model predicted an almost linear response up to about two-thirds of the failure load, followed by transition to plastic deformation. In contrast, the HASP model exhibited earlier stiffness reduction and more pronounced nonlinearity near failure, providing a closer match to the measured settlement curve in the final loading phase of the Footing A. For the Footing B, however, the HASP model overestimated settlements for the applied load increments, likely due to the early development of plastic strains from the onset of loading.

Figure 6 illustrates the general load-displacement behaviour predicted by the HASP and MCC models up to the adopted failure criterion, defined as a settlement equal to 20% of the footing width [31]. The MCC model predicts a higher ultimate bearing capacity, approximately 15% greater than that obtained with the HASP model, owing to its large purely elastic region within the initial yield surface. As a result, the stress path remains elastic over a wide range of loading.

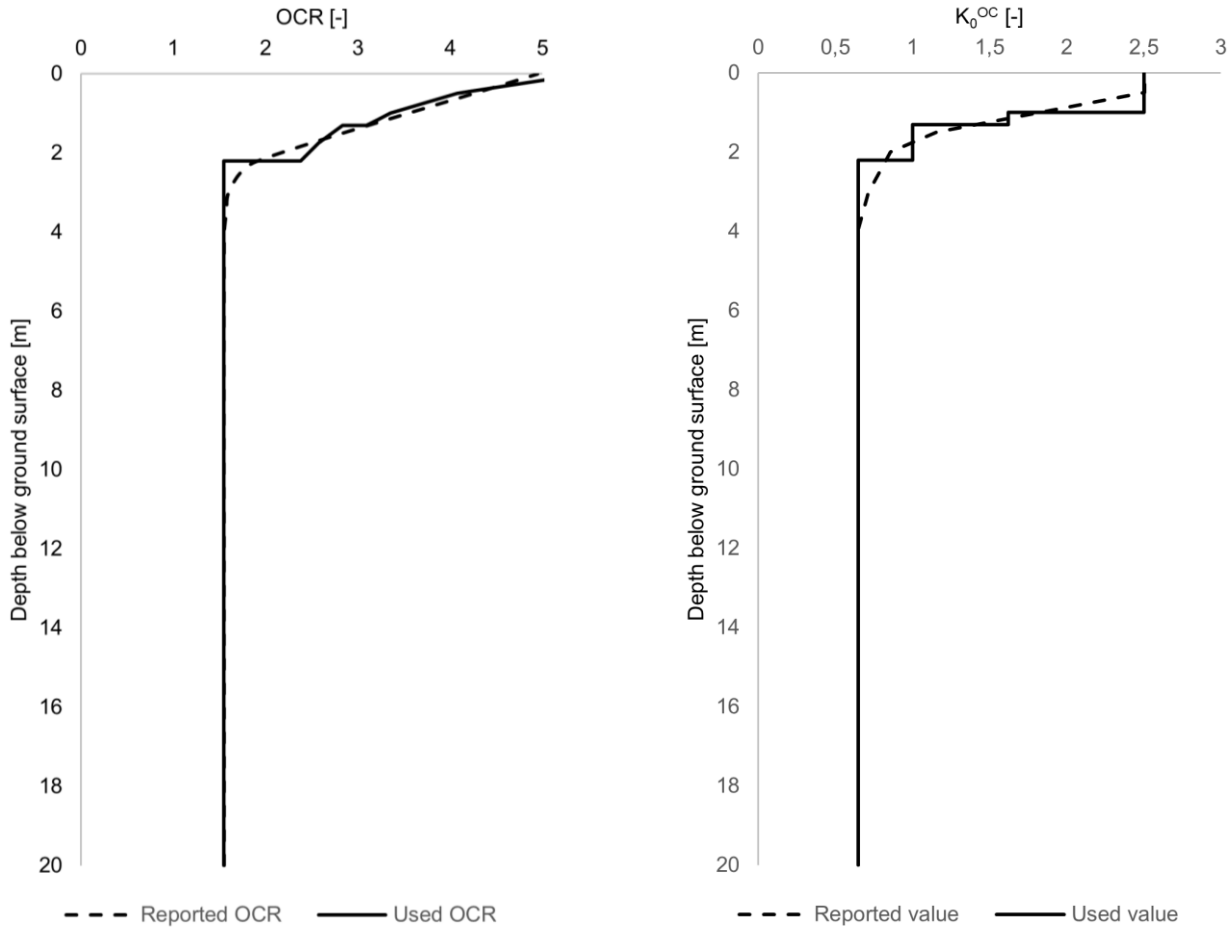

Figure 3. Variation of OCR and K_0^{OC} with depth

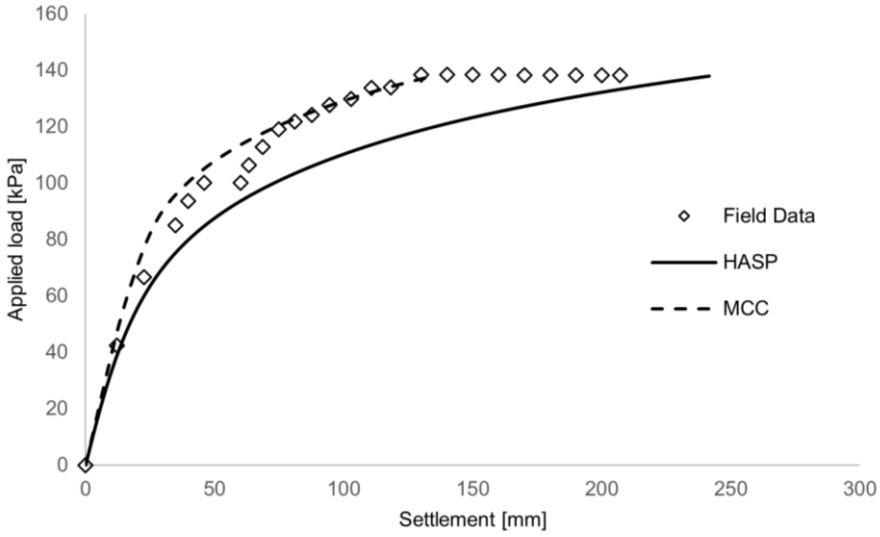

Figure 4. Load-displacement curves, Footing A

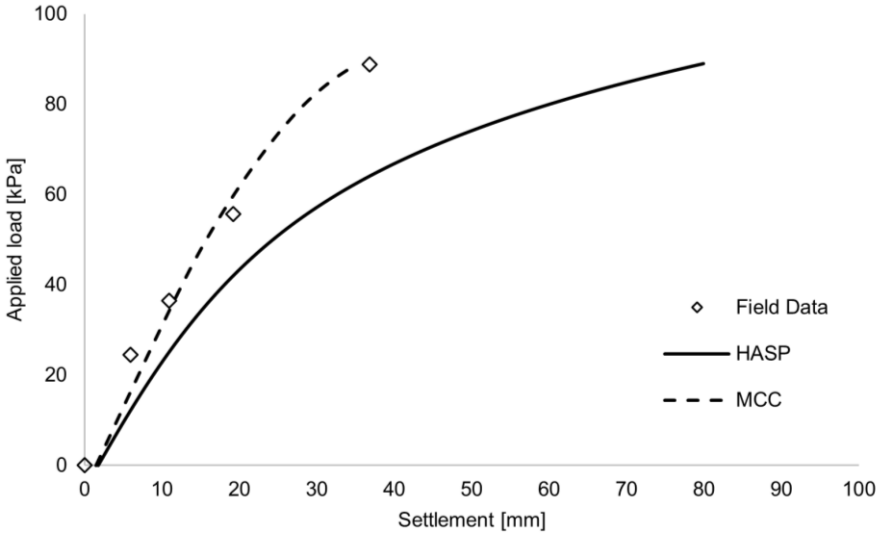

Figure 5. Load-displacement curves, Footing B

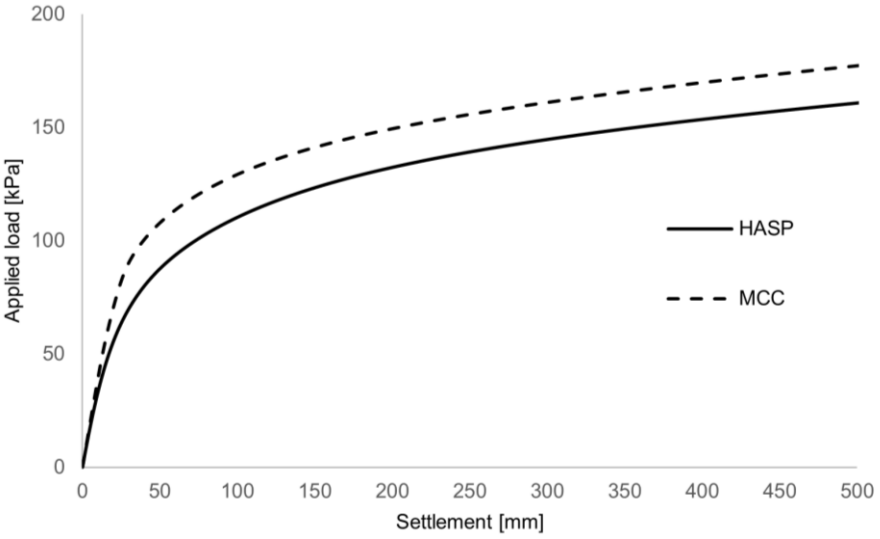

Figure 6. Load-displacement curves up to the failure

4.2 Footing settlement

Figure 7 presents the time-settlement response of the Footing B under maintained loading. Both constitutive models successfully reproduced the initial stiffness during the loading stage, accurately capturing both the initial rate of deformation and the gradual reduction in settlement rate with time. However, the HASP model provided a more accurate representation of the gradual increase in settlement over time under constant load. While the MCC model predicted relatively rapid stabilization of settlements after the initial consolidation phase, the HASP model reflected the continued time-dependent deformation, leading to a settlement-time trend closer to the field observations.

4.3 Pore-water pressures

A series of piezometers installed beneath Footings A and B recorded the evolution of excess pore-water pressures during and after loading. Owing to the similar loading conditions, only the results for the Footing B are discussed here. The variation of pore-water pressure with time was measured at five depths, and the results are compared with the numerical predictions obtained from the HASP model. The excess pore-water pressure developed at a given depth primarily depends on the applied stress increment and the local drainage conditions. At shallow depths, the applied stress increments were greater, resulting in higher initial excess pore pressures. However, dissipation occurred more rapidly due to the proximity of the drainage boundary at the base of the footing. With increasing depth, the rate of dissipation decreased, consistent with the longer drainage paths observed in the field.

The comparison between the measured and predicted excess pore-water pressures highlights the sensitivity of the results to the assumed permeability of the Bothkennar clay. In the original study, Freitas et al. [8] used a coefficient of permeability of the order of magnitude of 10^{-9} m/s, as shown in Table 1, but also noted that this value was likely too low to represent the in-situ conditions and that the field permeability might be significantly higher. When this value was adopted in the present analyses, the predicted excess pore pressures exceeded the field data and dissipated at a much slower rate, indicating unrealistically low drainage capacity (Figure 8).

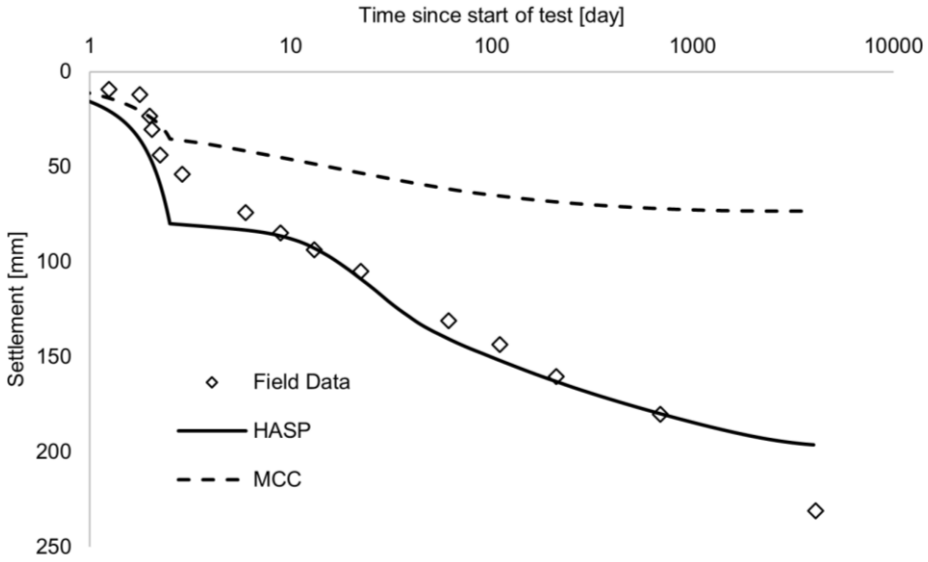

Figure 7. Time-settlement response of the Footing B

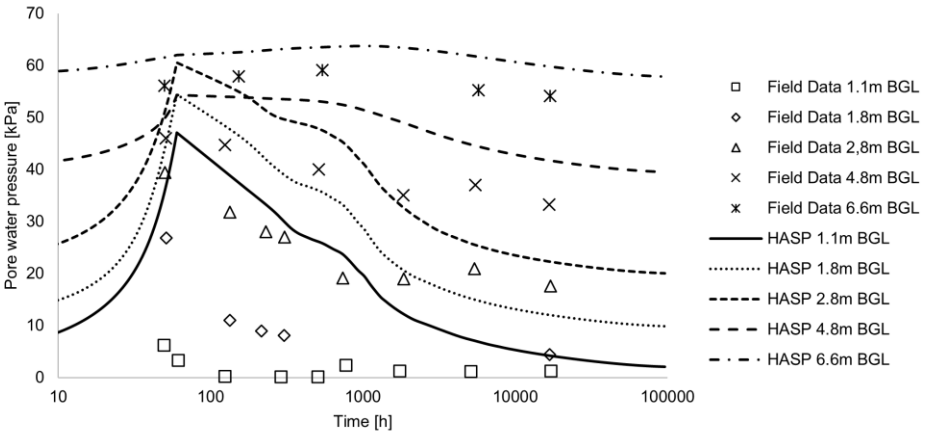

Figure 8. Excess pore-water pressure variation with time for the Footing B, k (m/s) from Table 1

Based on these observations, a parametric analysis was performed in which the permeability of all soil layers was uniformly increased to 10^{-7} m/s, consistent with the higher field permeability reported for the Bothkennar formation. With this modification, the predicted pore-water pressures and their dissipation rate showed excellent agreement with the field measurements (Figure 9), confirming that the lower permeability value used in previous analyses likely underestimated the actual drainage behaviour of the foundation clay.

4.4 Horizontal movements

Horizontal displacements beneath the Footing B were monitored using two inclinometers, I1 and I2, positioned 0.15 m from the footing edge on opposite sides. The inclinometer readings were taken periodically during the loading phase. The measured and predicted profiles of lateral movement with depth are compared in Figures 10 and 11. It should be noted that the measured horizontal movements differ between Inclinometers I1 and I2 despite their symmetric installation. This asymmetry is consistent with the field observations reported by Freitas et al. [8], who documented a pronounced tilt of the Footing B developing from the early loading stages. As a consequence, lateral movements were significantly larger on the side monitored by Inclinometer I2 than on the opposite side, explaining the higher measured displacements.

Both constitutive models reproduced the overall shape of the displacement profiles, with maximum horizontal movement occurring at a depth of about 1.5 m below the footing base, consistent with the field observations. For Inclinometer I1, the MCC model provided a closer match to the recorded values (Figure 10), whereas the HASP model tended to overpredict the magnitude of horizontal displacement. In contrast, for Inclinometer I2 (Figure 11), the HASP model reproduced the measured profile and displacement magnitude very accurately, while the MCC model underestimated lateral movements.

5 Conclusions

This paper presented a comprehensive numerical study of shallow foundations on overconsolidated clays, based on field observations from the Bothkennar research site. The analyses were performed using the HASP model implemented in PLAXIS 2D as a user-defined constitutive formulation within the critical state framework. The model parameters were adopted directly from published laboratory data, without any additional calibration, to evaluate the predictive capability of the constitutive formulation under realistic conditions. The numerical simulations reproduced both short-term and long-term field tests on two instrumented footings. The predicted load-displacement relationships captured the measured trends, showing a progressive reduction of stiffness and a nonlinear response at higher load levels consistent with field behaviour. The analysis of time-dependent settlements indicated that continued deformation occurs even under constant loading, governed by pore-pressure dissipation and the gradual readjustment of the effective stress state. The comparison between measured and computed excess pore-water pressures showed good agreement when a realistic permeability value was adopted. The observed correspondence between predicted and measured responses suggests that these coupled mechanisms can be effectively represented by an elasto-plastic formulation when realistic permeability and consolidation parameters are applied. The results confirm that advanced numerical modelling provides a robust and practical framework for analysing the hydro-mechanical response of overconsolidated clays. However, the long-term deformation behaviour of overconsolidated clays is also influenced by time-dependent processes not explicitly considered in the present analyses. To improve the prediction of delayed settlements and viscous strain accumulation, future research should focus on implementing a creep law that allows the consideration of nonlinear creep effects. Such an extension would enable a more complete representation of soil behaviour under sustained loading and provide a more reliable basis for evaluating both the bearing capacity and long-term serviceability of foundations on overconsolidated clays.

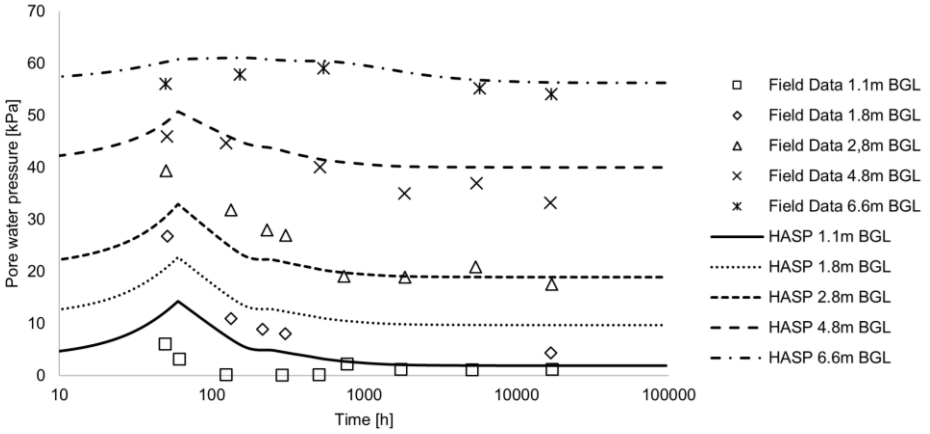

Figure 9. Excess pore-water pressure variation with time for Footing B, k=10^{-7} m/s

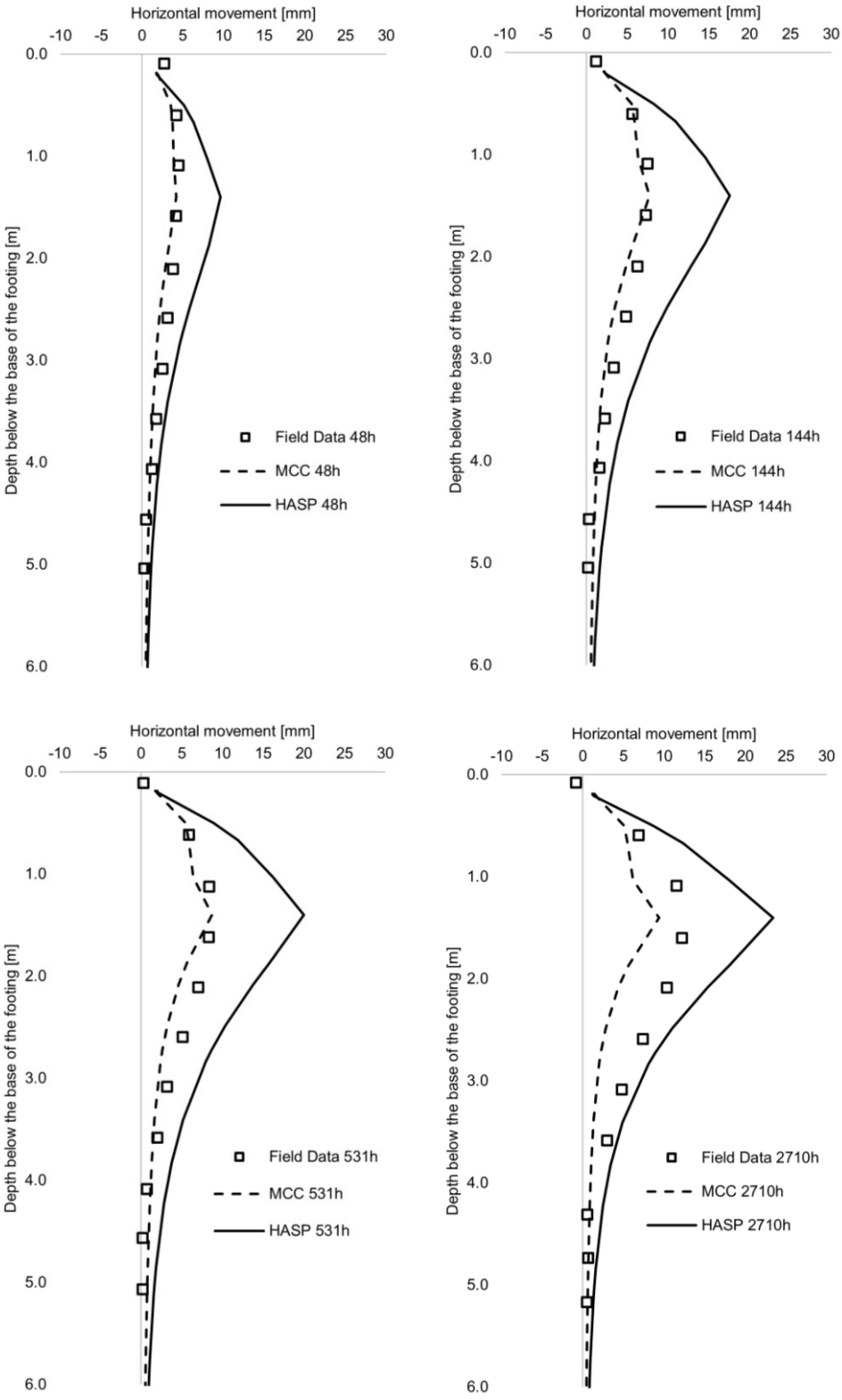

Figure 10. Horizontal displacements over time, inclinometer I1, Footing B

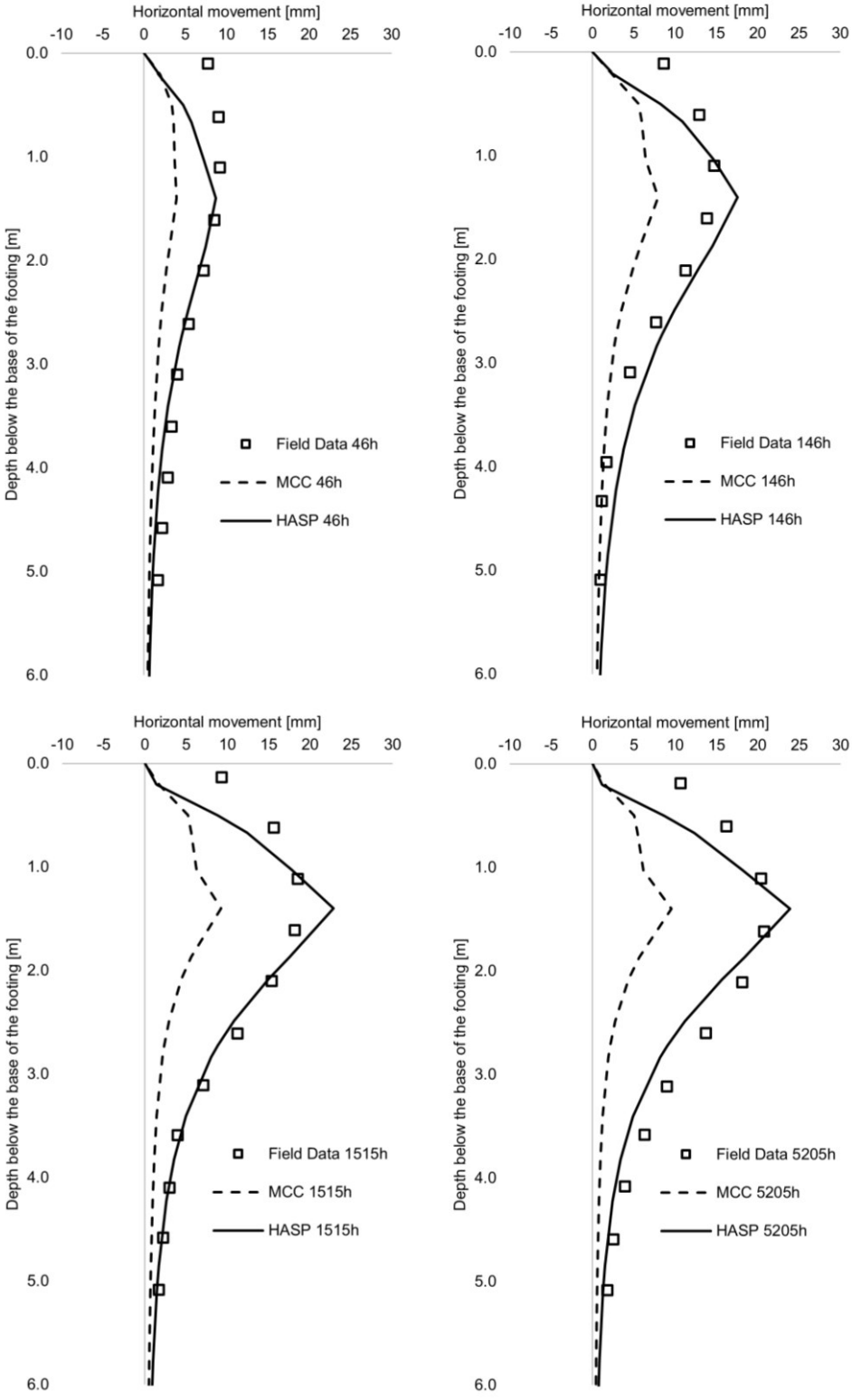

Figure 11. Horizontal displacements over time, inclinometer I2, Footing B

CRediT authorship contribution statement

Nikola Obradović: Conceptualization, Investigation, Methodology, Software, Writing – original draft. Sanja Jocković: Conceptualization, Methodology, Supervision, Writing – review & editing.

Declaration of competing interest

The authors declare that they have no known competing financial interests or personal relationships that could have appeared to influence the work reported in this paper.

Acknowledgement

This research was partially supported by the Serbian Ministry of Science, Technological Development and Innovation via the Project 200092.

References

[1] J.H. Atkinson, P.L. Bransby, *The Mechanics of Soils: An Introduction to Critical State Soil Mechanics*, McGraw-Hill, London, 1977.
[2] J.B. Burland, On the compressibility and shear strength of natural clays, *Géotechnique* 40 (3) (1990) 329–378.
[3] J.H. Atkinson, G. Sallfors, Experimental determination of stress–strain–time characteristics in laboratory and in situ tests. General report to Session 1, *Proceedings of the 10th European Conference on Soil Mechanics and Foundation Engineering*, Florence, vol. 3 (1991) 915–956.
[4] D.M. Potts, L. Zdravković, *Finite Element Analysis in Geotechnical Engineering: Theory*, Thomas Telford Ltd., London, 1999.
[5] D.M. Potts, L. Zdravković, *Finite Element Analysis in Geotechnical Engineering: Application*, Thomas Telford Ltd., London, 2001.
[6] M. Budhu, Design of shallow footings on heavily overconsolidated clays, *Can. Geotech. J.* 49 (2) (2012) 184–196.
[7] T.M.B. Freitas, D.M. Potts, L. Zdravković, The effect of creep on the short-term bearing capacity of pre-loaded footings, Comput. Geotech. 42 (2012) 99–108.
[8] T.M.B. Freitas, D.M. Potts, L. Zdravković, Numerical study on the response of two footings at Bothkennar research site, Géotechnique 65 (3) (2015) 155–168.
[9] M. López, M. Sanchez, J.C. Santamarina, Modeling of settlement and bearing capacity of shallow foundations in overconsolidated clays, *Journal of GeoEngineering* 17 (1) (2022) 24–33.
[10] R.J. Jardine, The 6th ISSMGE McClelland Lecture: Time-dependent vertical bearing behaviour of shallow foundations and driven piles, in: *SUT Offshore Site Investigation and Geotechnics Conference Proceedings*, Society for Underwater Technology (SUT), London, September 2023, pp. SUT-OSIG
[11] B. Schneider-Muntau, I. Bathaeian, Simulation of settlement and bearing capacity of shallow foundations with soft particle code (SPARC) and FE, *GEM – Int. J. Geomath.* 9 (2018) 359–375.
[12] A. Goh, R. Zhang, W. Wang, L. Wang, H. Liu, W. Zhang, Numerical study of the effects of groundwater drawdown on ground settlement for excavation in residual soils, *Acta Geotech.* 15 (6) (2020) 1259–1272.
[13] N. Obradović, S. Jocković, M. Vukićević, Application of hardening state parameter constitutive model for prediction of overconsolidated soft clay behavior due to embankment loading, *Appl. Sci.* 13 (4) (2023) 2175.
[14] A.N. Schofield, C.P. Wroth, Critical State Soil Mechanics, McGraw-Hill, London, 1968.
[15] K.H. Roscoe, J.B. Burland, On the generalised stress–strain behaviour of 'wet' clay, in: J. Heyman, F.A. Leckie (Eds.), *Engineering Plasticity*, Cambridge University Press, Cambridge, UK, 1968, pp. 535–609.
[16] A. Al-Tabbaa, D.M. Wood, An experimentally based "bubble" model for clay, in: S. Pietruszczak, G.N. Pande (Eds.), *Numerical Models in Geomechanics – NUMOG III*, Elsevier Applied Science, London, 1989, pp. 91–99.
[17] A. Whittle, M. Kavvadas, Formulation of MIT-E3 constitutive model for overconsolidated clays, *J. Geotech. Eng.* 120 (1) (1994) 173–198.
[18] S.E. Stallebrass, R.N. Taylor, The development of a constitutive model for the prediction of ground movements in overconsolidated clay, *Géotechnique* 47 (1997) 235–253.
[19] A. Gajo, D.M. Wood, A new approach to anisotropic, bounding surface plasticity: general formulation and simulations of natural and reconstituted clay behaviour, *Int. J. Numer. Anal. Methods Geomech.* 25 (3) (2001) 207–241.
[20] H.S. Yu, CASM: a unified state parameter model for clay and sand, *Int. J. Numer. Anal. Methods Geomech.* 22 (8) (1998) 621–653.
[21] G.R. McDowell, K.W. Hau, A simple non-associated three-surface kinematic hardening model, *Géotechnique* 53 (4) (2003) 433–437.
[22] Y.F. Dafalias, M.T. Manzari, A.G. Papadimitriou, SANICLAY: simple anisotropic clay plasticity model, *Int. J. Numer. Anal. Methods Geomech.* 30 (2006) 1231–1257.
[23] Y.P. Yao, W. Hou, A.N. Zhou, UH model: three-dimensional unified hardening model for overconsolidated clays, *Géotechnique* 59 (2009) 451–469.
[24] S. Jocković, *Formulation and implementation of a constitutive model for overconsolidated clays*, PhD Thesis, University of Belgrade, Faculty of Civil Engineering, Belgrade, 2017.
[25] S. Jocković, M. Vukićević, Bounding surface model for overconsolidated clays with new state parameter formulation of hardening rule, *Comput. Geotech.* 83 (2017) 16–29.
[26] N. Obradović, *Development of the "HASP" constitutive model for overconsolidated clays with application in finite element analysis*, PhD Thesis, University of Belgrade, Faculty of Civil Engineering, Belgrade, 2024.
[27] S. Jocković, M. Vukićević, Validation and implementation of HASP constitutive model for overconsolidated clays, *Građev. Mater. Konstrukc.* 61 (1) (2018) 91–109.
[28] S. Sloan, A. Abbo, D. Sheng, Refined explicit integration of elastoplastic models with automatic error control, *Eng. Comput.* 18 (1) (2001) 121–194.
[29] R.J. Jardine, B.M. Lehane, P.R. Smith, P.A. Gildea, Vertical loading experiments on rigid pad foundations at Bothkennar, *Géotechnique* 45 (4) (1995) 573–597.
[30] D.F.T. Nash, G.C. Sills, L.R. Davison, One-dimensional consolidation testing of soft clay from Bothkennar, *Géotechnique* 42 (2) (1992) 241–256.
[31] A.S. Vesic, Analysis of ultimate loads of shallow foundations, J. Soil Mech. Found. Div., ASCE 99 (SM1) (1973) 45–73.